

CASE REPORT

Open Access



Ectopic parathyroid adenoma: successful localization with ¹⁸F-fluorocholine PET/CT and parathyroid venous sampling in two cases

Byungkwan Jung¹ , Yoochan Shin¹, Sungahn Lee¹, Namki Hong², Sang Yu Nam^{3*} and Sihoon Lee^{1*}

Abstract

Background Clinically suspected parathyroid adenomas, which are not localized by conventional imaging such as ultrasonography and technetium-99 m (99mTc) sestamibi scintigraphy, remain challenging. We describe two patients with hypercalcemia and elevated parathyroid hormone (PTH) levels, in whom ultrasonography or technetium-99 m sestamibi scintigraphy failed to identify the lesions. Both were successfully localized by novel combined use of fluorine 18 (¹⁸F) fluorocholine positron emission tomography/computed tomography (FCH PET/CT) in conjunction with parathyroid venous sampling (PVS).

Case presentation In the first case of 59 year-old Korean man with diabetes, a 2.0-cm mass in the left mediastinum was identified and removed via thoracoscopic robotic excision, with histopathology confirming an ectopic parathyroid adenoma. Postoperatively, serum calcium, PTH and creatinine levels improved, and the patient's daily insulin requirement decreased from 90 to 15 units. In the second case of 55 year-old Korean woman, a 0.8-cm nodule was localized in the retropharyngeal space posterior to the right pyriform sinus. Due to the deep location and high surgical risk, the patient was managed non-surgically with annual intravenous bisphosphonate to control hypercalcemia and prevent bone loss.

Conclusions These cases highlight the diagnostic value of FCH PET/CT and PVS for precise localization of parathyroid adenomas not detectable by first-line imaging, enabling optimal management and potentially improving outcomes beyond calcium and bone metabolism, including renal function and glucose homeostasis. To the best of our knowledge, this is the first case report demonstrating the clinical advantage of the combined use of FCH PET/CT and PVS.

Clinical trial number Not applicable

Keywords Primary hyperparathyroidism, Ectopic parathyroid adenoma, ¹⁸F fluorocholine PET/CT, Parathyroid venous sampling, Insulin resistance

*Correspondence:
Sang Yu Nam
sy.nam@gilhospital.com
Sihoon Lee
shleemd@gachon.ac.kr

¹Laboratory of Genomics and Translational Medicine, Department of Internal Medicine, Gil Medical Center, Gachon University College of Medicine, Incheon, Korea

²Department of Internal Medicine, Yonsei University College of Medicine, Seoul, Korea

³Department of Radiology, Gil Medical Center, Gachon University College of Medicine, Incheon, Korea



© The Author(s) 2025. **Open Access** This article is licensed under a Creative Commons Attribution-NonCommercial-NoDerivatives 4.0 International License, which permits any non-commercial use, sharing, distribution and reproduction in any medium or format, as long as you give appropriate credit to the original author(s) and the source, provide a link to the Creative Commons licence, and indicate if you modified the licensed material. You do not have permission under this licence to share adapted material derived from this article or parts of it. The images or other third party material in this article are included in the article's Creative Commons licence, unless indicated otherwise in a credit line to the material. If material is not included in the article's Creative Commons licence and your intended use is not permitted by statutory regulation or exceeds the permitted use, you will need to obtain permission directly from the copyright holder. To view a copy of this licence, visit <http://creativecommons.org/licenses/by-nc-nd/4.0/>.

Background

Primary hyperparathyroidism (PHPT), most often attributed to a solitary parathyroid adenoma ($\approx 80\%$), has been increasingly diagnosed with the widespread use of biochemical screening [1]. While often asymptomatic, PHPT can present with nephrolithiasis ($< 20\%$), bone disease, and metabolic disturbances including impaired glucose regulation [1, 2]. Chronic hypercalcemia, a hallmark of PHPT, contributes to kidney stone formation and progressive renal impairment [3].

Minimally invasive parathyroidectomy, dependent on accurate preoperative localization of hyperfunctioning parathyroid tissue, has become the standard surgical approach for PHPT in most centers owing to its superior surgical outcomes compared to cervical exploration [4]. Conventional imaging modalities include ultrasonography and technetium-99 m (99mTc) sestamibi (MIBI) scintigraphy, commonly referred to as the MIBI scan. However, both modalities demonstrate only moderate sensitivity – 76.1% (95% confidence interval [CI], 70.4–81.4%) for ultrasonography and 78.9% (95% CI, 64–90.6%) for MIBI SPECT (Single-Photon Emission Computed Tomography) – as reported in a meta-analysis [5]. In addition, ultrasonography and MIBI scan showed a discordance rate of 28.3% in a single-center study [6].

Fluorine 18 (^{18}F) fluorocholine positron emission tomography/computed tomography (FCH PET/CT) has recently emerged as a highly sensitive imaging modality, with a pooled detection rate of 97% reported in a systematic review [7]. Its uptake may reflect increased phospholipid synthesis and choline metabolism in hyperfunctioning parathyroid tissue [8]. Complementally, Parathyroid Venous Sampling (PVS) is an invasive catheter-based procedure that measures direct PTH gradients across specific venous drainage sites [9].

Herein, we present two patients with ectopic parathyroid adenoma, not localized by conventional imaging

with ultrasonography and MIBI scan, but successfully localized by FCH PET/CT and PVS. To the best of our knowledge, no reports have demonstrated the combined use of FCH PET/CT and PVS.

Case presentation

Patient 1 (Pt #1)

A 59-year-old Asian man with a medical history of type 2 diabetes, hypertension, and diabetic kidney disease (stage 4) was referred to our clinic in July 2019 with the chief complaint of elevated HbA1c levels. During a follow-up visit in June 2021, hypercalcemia was first noted with elevated PTH levels, and subsequent laboratory analyses revealed increases in serum calcium, PTH and creatinine levels (Table 1). His complete blood cell count, cholesterol, ions, and other biomarker levels were within the normal range, and no significant family history was found. Dual-energy X-ray absorptiometry (DEXA) bone scan results were normal.

Patient 2 (Pt #2)

A 55-year-old Asian woman previously diagnosed with papillary thyroid carcinoma underwent right unilateral thyroid lobectomy. Post-lobectomy follow-up demonstrated elevated serum calcium and PTH levels.

Informed consents for publication of clinical data were obtained from the study participants.

Localization of parathyroid adenoma

For both patients, persistent hypercalcemia with elevated PTH level and normal phosphate levels raised suspicion of primary hyperparathyroidism rather than secondary disease. Initial localization studies using thyroid ultrasonography and MIBI SPECT/CT (Single-Photon Emission Computed Tomography/Computed Tomography) were conducted to detect PTH producing tissue. In Pt #1, ultrasonography revealed a 0.5-cm oval isoechoic benign

Table 1 Serial laboratory analysis changes of Pt #1

Test items	Reference range	Unit	2 years before diagnosis of PHPT	Initial diagnosis of PHPT	7 weeks before parathyroidectomy	2 weeks after parathyroidectomy
Calcium, serum	8–10 (2.00–2.50)	mg/dL (mmol/L)	9.69 2.42	10.79 2.69	10.96 2.73	9.18 2.29
Ionized calcium, serum	4.21–5.41 (1.05–1.35)	mg/dL (mmol/L)	5.21 1.3	5.85 1.46	5.93 1.48	5.01 1.25
Parathyroid hormone, serum	10–55 (1.1–5.8)	pg/mL (pmol/L)	68.5 7.3	164.5 17.4	151.4 16.1	69 7.3
Creatinine, serum	0.6–1.2 (0.05–0.1)	mg/dL (mmol/L)	1.41 0.12	3.44 0.31	3.38 0.3	2.42 0.21
Phosphorus, serum	2.3–4.7 (0.7–1.5)	mg/dL (mmol/L)	3.36 1.08	3.9 1.26	3.49 1.13	3.16 1.02
HbA1c, serum	4.0–5.7	%	8.8	11.2	8.7	7.2

Abnormal values are shown in bold

nodule in the middle of the right lobe, and a 0.5-cm benign spongiform nodule on the lower pole of the right lobe. MIBI SPECT/CT revealed only subtle sestamibi-retaining areas, which are inconclusive because of low uptake, absence of focal localization, and no corresponding anatomical lesion on ultrasound (Fig. 1). Unconvincing results from first-line localization methods required referral to a specialized parathyroid center to perform additional diagnostic modalities including FCH PET/CT and PVS. The FCH PET/CT images showed concentrated FCH uptake in the anterior mediastinum (Fig. 2). According to PVS, increased ratios of PTH compared to the peripheral levels were observed in the upper superior vena cava (SVC) (1.64-fold), middle SVC (1.63-fold), and lower SVC (1.47-fold), indicating an ectopic parathyroid adenoma (EPA) located under the thyroid, closer to the thoracic region (Fig. 3). Concordant findings from both PVS and FCH PET/CT strongly suggested EPA in the anterior mediastinum.

In **Pt #2**, MIBI SPECT/CT could not successfully localize the PTH-producing tissue (Fig. 1). Then, PVS performed in a specialized parathyroid center showed a 6.51-fold increase in PTH level at right lower internal

jugular vein (IJV), and a 2.71-fold increase at the right convergence of the IJV and brachiocephalic vein (BCV) (Fig. 3). FCH PET/CT identified a 0.4×0.8 cm-sized lesion in the retropharyngeal area posterior to the right pyriform sinus (Fig. 2), which anatomically corresponds to venous drainage territory of the right IJV. Concordance between imaging and sampling data strongly suggested an EPA.

Treatment and outcome

In **Pt #1**, minimally invasive parathyroidectomy through robot-assisted thoracoscopic excision was performed. Pathological analysis confirmed EPA diagnosis, with diffuse weakly positive PTH immunohistochemical staining. Postoperative laboratory analysis demonstrated normalization of both serum calcium and PTH levels (Table 1). HbA1c decreased markedly from 8.7% to 7.2% (reference range : 4.0–5.7%), accompanied by substantial reduction in insulin requirements from 48 international unit (IU) and 42 IU twice daily to 15 IU once daily. Serum creatinine levels also declined, indicating improved renal function. These findings suggest a potential favorable

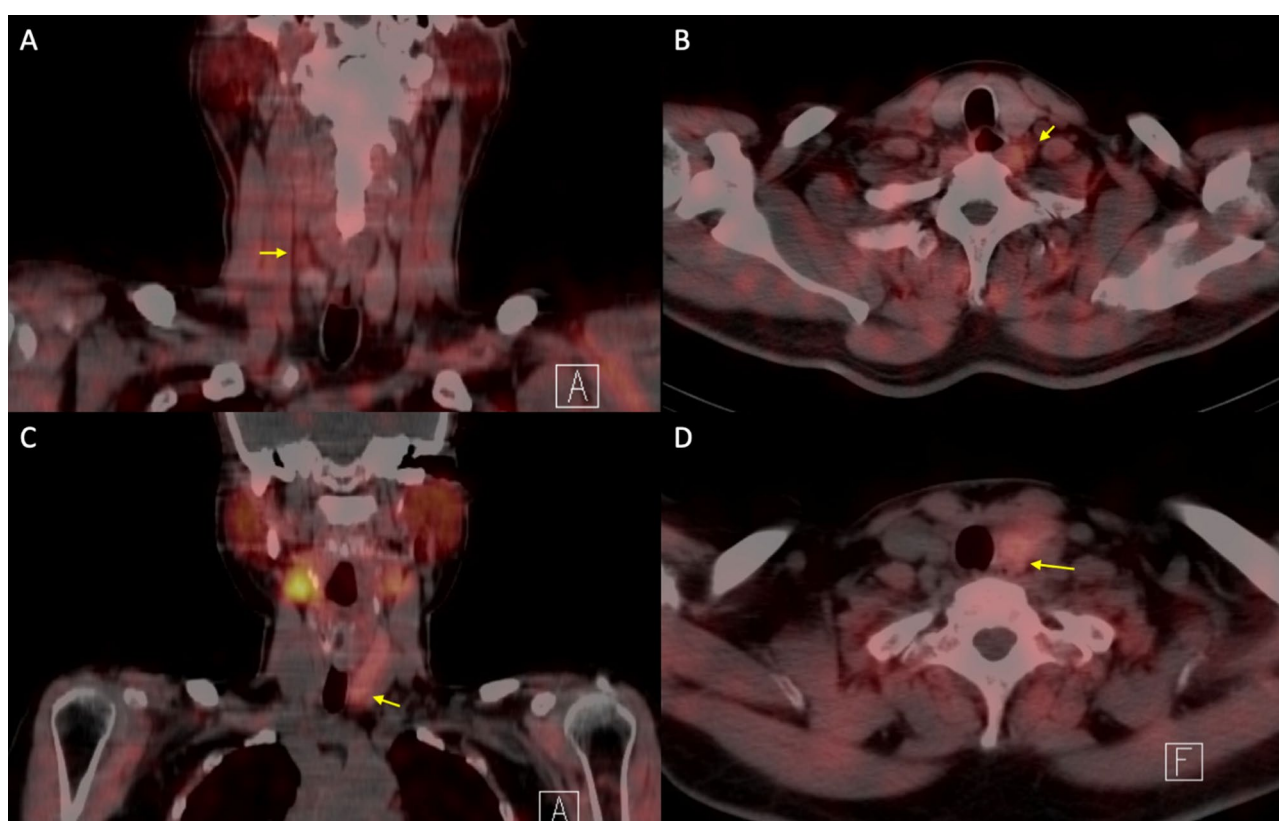


Fig. 1 Technetium-99 m (99mTc) sestamibi (MIBI) SPECT/CT (Single-Photon Emission Computed Tomography/Computed Tomography) of **Pt #1** in (A) coronal and (B) axial view, and **Pt #2** in (C) coronal and (D) axial view. The arrow in (A) indicates subtle sestamibi-retaining area posterior to the right upper lobe, and that of (B) indicates the other posterior to the middle of the left lobe of **Pt #1**. Arrows in (C) and (D) indicate subtle sestamibi-retaining area at the lower posterior area of left thyroid of **Pt #2**. These regions were initially interpreted as areas of faint sestamibi uptake on the primary MIBI SPECT/CT reading but were considered inconclusive due to the lack of definite focal localization and discordance with ultrasonography findings

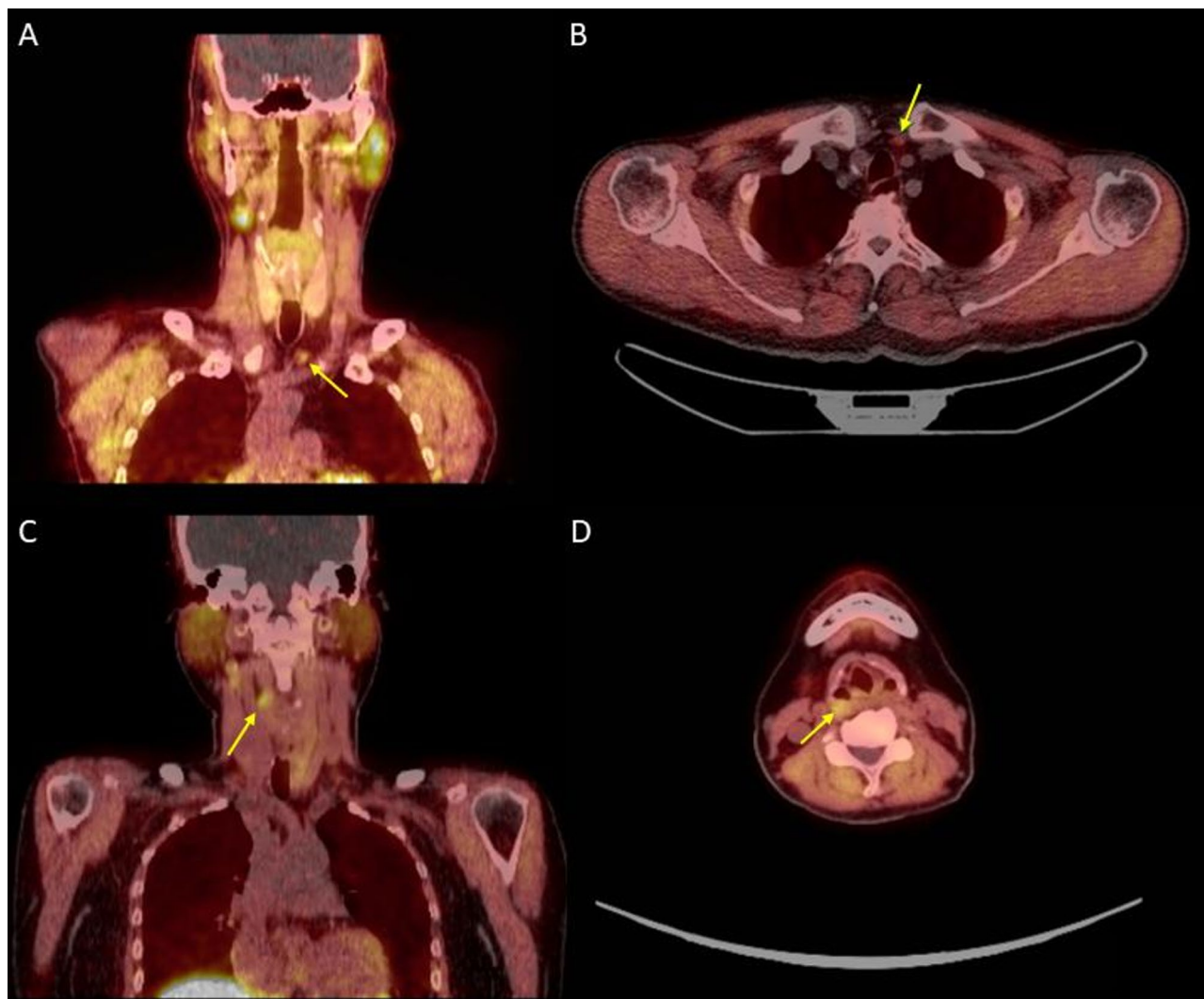


Fig. 2 Fluorine 18 (^{18}F) fluorocholine positron emission tomography/computed tomography (FCH PET/CT) of **Pt #1** in (A) coronal and (B) axial view, and **Pt #2** in (C) coronal and (D) axial view. Arrows in (A) and (B) indicate ectopic parathyroid adenoma in the anterior mediastinum of **Pt #1**. Arrows in (C) and (D) indicate a 0.4×0.8 cm-sized ectopic parathyroid adenoma in the retropharyngeal area posterior to the right pyriform sinus of **Pt #2**

association between reduced PTH levels, improved insulin sensitivity, and enhanced renal function.

In **Pt #2**, surgical excision was deferred because of the deep anatomical location of the EPA and associated high surgical risk. Instead, the patient was managed conservatively with calcium and vitamin D supplements, along with annual intravenous zoledronate, a potent bisphosphonate, not only to prevent osteoporosis secondary to chronic PTH production, but also to mitigate hypercalcemia. Over 4 years of follow-up, serum calcium remained mildly elevated while PTH levels gradually declined. Renal function was stable, and bone mineral density at the lumbar spine improved from a T-score of -1.5 to -0.7 , indicating effective skeletal protection with annual zoledronate therapy despite persistent hypercalcemia (Table 2).

Discussion and conclusions

In both cases, the EPA, undetected by conventional ultrasound or MIBI scan, was accurately localized using FCH PET/CT combined with PVS. FCH PET/CT offers superior sensitivity and spatial resolution. After the definite lesions were localized, the previously acquired MIBI scan were retrospectively reviewed to reassess concordance with the imaging findings. As shown in Fig. 4, subtle sestamibi uptake could be observed on MIBI SPECT/CT, but these findings were far less definite than those on FCH PET/CT.

PVS offers objective biochemical evidence of hormone secretion, complementing imaging, which relies on radiotracer uptake and influenced by factors such as gland size, background activity, and anatomical distortion. Accurate preoperative localization, as shown in **Pt #1**, enables minimally invasive parathyroidectomy and

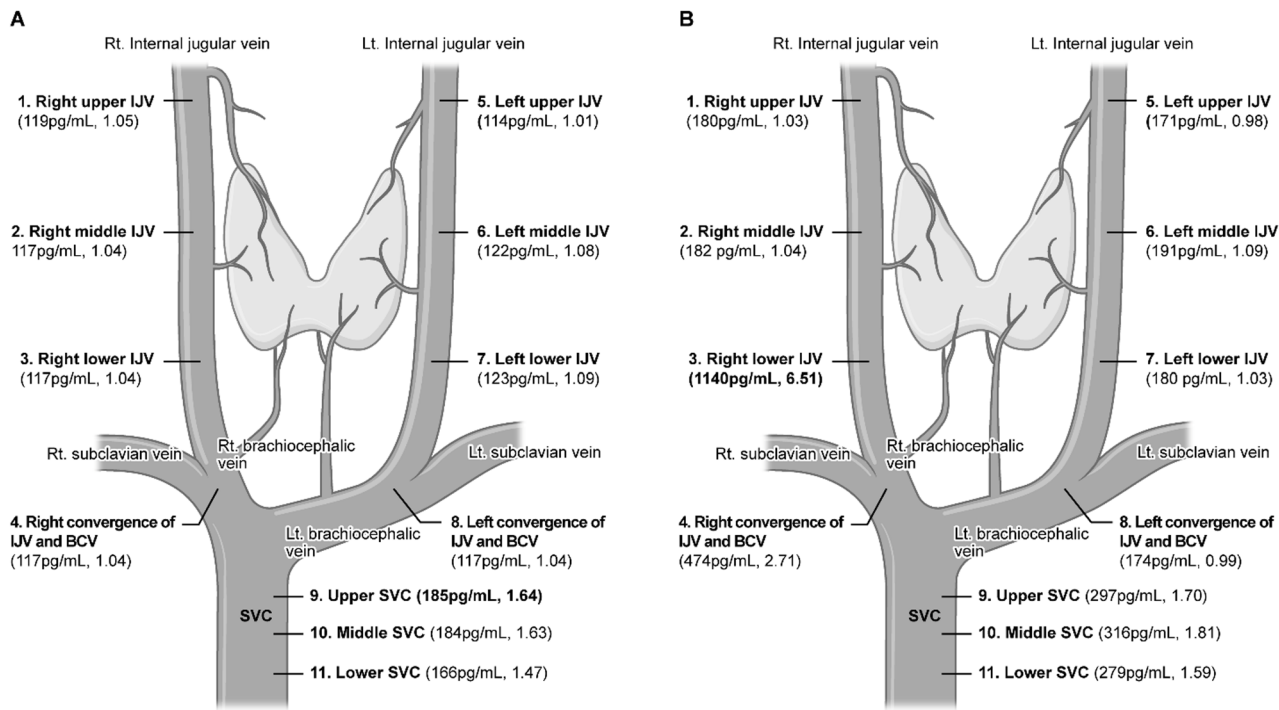


Fig. 3 Parathyroid Venous Sampling (PVS) results of Pt #1 (A) and Pt #2 (B). Each location is labeled with its corresponding parathyroid hormone (PTH) level and ratio to the peripheral PTH level (reference range: 10–55 pg/mL [1.1–5.8 pmol/L] of both patients). The peripheral PTH levels of Pt #1 and Pt #2 are 113.00 pg/mL [12.0 pmol/L] and 175.00 pg/mL [18.6 pmol/L], respectively. In Pt #1 (A), increased ratios of PTH compared to the peripheral levels were observed in the upper superior vena cava (SVC) (1.64-fold), highlighted in bold, middle SVC (1.63-fold), and lower SVC (1.7-fold), indicating an ectopic parathyroid adenoma (EPA) located under the thyroid, closer to the thoracic region. In Pt #2 (B), a 6.51-fold increase in PTH level at right lower internal jugular vein (IJV), highlighted in bold, and a 2.71-fold increase at right convergence of the IJV and brachiocephalic vein (BCV), indicating an EPA located in closer to the right pyriform sinus

Table 2 Serial laboratory analysis changes of Pt #2

Test items	Reference range	Unit	Initial diagnosis of PHPT	1 year after diagnosis	4 years after diagnosis
Calcium, serum	8–10 (2.00–2.50)	mg/dL (mmol/L)	9.42 2.35	10.94 2.73	11.1 2.77
Ionized calcium, serum	4.21–5.41 (1.05–1.35)	mg/dL (mmol/L)	5.45 1.36	5.93 1.48	5.81 1.45
Parathyroid hormone, serum	10–55 (1.1–5.8)	pg/mL (pmol/L)	386.6 40.6	184.8 19.4	136.2 14.3
Creatinine, serum	0.6–1.2 (0.05–0.1)	mg/dL (mmol/L)	0.61 54	0.77 68	0.92 81
Phosphorus, serum	2.3–4.7 (0.7–1.5)	mg/dL (mmol/L)	2.82 0.91	2.79 0.9	2.29 0.74
BMD (T-score, L1-L3)	≥-1.0		-1.5	-1.3	-0.7

Abnormal values are shown in bold

definitive cure of PHPT. When lesions are not identified, exploratory surgery may be performed, achieving a high cure rate [10]. However, it is technically demanding, usually limited to high-volume centers, and associated with less favorable outcomes compared with minimally invasive surgery, including higher complication rates, longer operation time, extended hospital stay, and greater cost [4]. Our findings underscore the clinical value of advanced modalities such as FCH PET/CT combined

with PVS, which enhance lesion detection in ectopic or challenging cases and thereby facilitate minimally invasive surgery.

For EPAs at prohibitive surgical risk, as in Pt #2, medical therapy with calcium, vitamin D, and bisphosphonates may mitigate hypercalcemia. Bisphosphonate inhibits osteoclast-mediated bone resorption, thereby reducing calcium release from bone into the circulation and contributing to the correction of hypercalcemia.

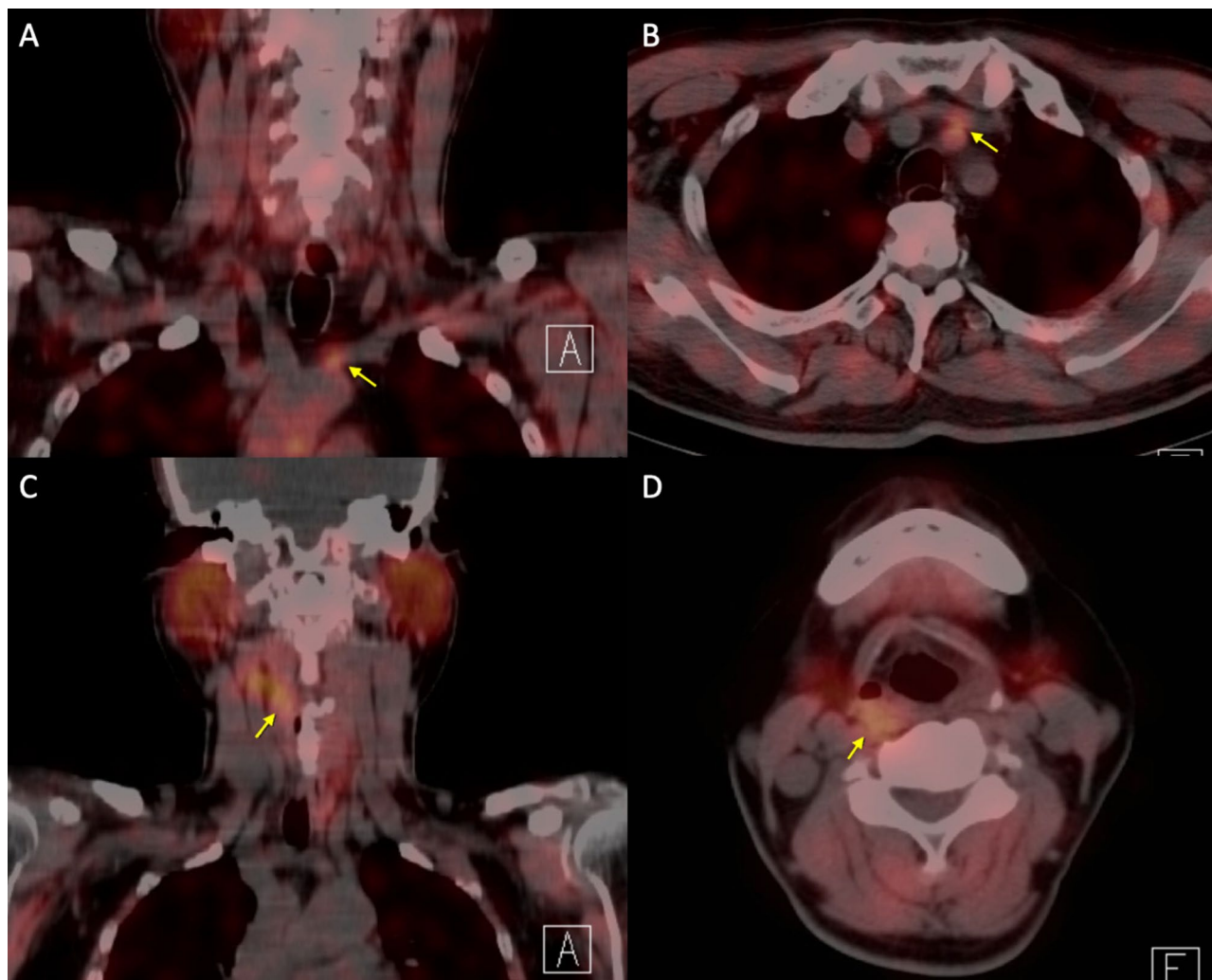


Fig. 4 Technetium-99 m (99mTc) sestamibi (MIBI) SPECT/CT (Single-Photon Emission Computed Tomography/Computed Tomography) of Pt #1 in (A) coronal and (B) axial view, and Pt #2 in (C) coronal and (D) axial view. Arrows show the areas that were later localized with Fluorine 18 (¹⁸F) fluorocholine positron emission tomography/computed tomography (FCH PET/CT), but not successfully localized by MIBI scan initially. Upon retrospective review, subtle uptake changes could be observed in these regions, although the findings were not as definite as those on FCH PET/CT

Parathyroidectomy generally provides superior long-term outcomes in fracture prevention and possibly renal preservation, although the latter remains debated [11–13]. The EPA in Pt #2 was located in the retropharyngeal space posterior to the right pyriform sinus, an extremely rare site with high surgical risk [14, 15]. In one reported case, transoral surgery was selected over a transcervical one due to the proximity of the recurrent laryngeal nerve [14]. For Pt #2, however, both approaches were infeasible, and surgery was not performed.

Growing evidence supports the high prevalence of glucose tolerance disorders and diabetes mellitus in patients with PHPT. Although the underlying mechanism remains unknown, one hypothesis is that insulin-stimulated glucose uptake is decreased as a result of increased calcium concentrations [2]. Another hypothesis suggests that a reduced phosphoric acid concentration

causes an imbalance in energy metabolism, resulting in increased insulin resistance [16]. Supporting research has demonstrated that parathyroidectomy reduces insulin resistance. According to Duran et al., after curative parathyroidectomy, serum levels of calcium ($p = 0.001$), PTH ($p < 0.001$), insulin ($p = 0.003$), and homeostatic model assessment of insulin resistance (HOMA-IR) ($p = 0.003$) decreased, whereas phosphorus levels ($p = 0.001$) increased two months after surgery. No changes in vitamin D or glucose levels were observed [17]. Similarly, Noghani et al. reported a reduced HOMA-IR in 51 of 65 patients after curative parathyroidectomy [18]. Although the underlying mechanisms differ, another report has suggested an association between elevated PTH levels and insulin resistance. Muniyappa et al. reported that patients with pseudohypoparathyroidism type 1a (PHP1a), who exhibit end-organ resistance to high PTH,

are insulin resistant and are at a higher risk of diabetes mellitus compared with healthy individuals of the same age and degree of adiposity [19].

Improved renal function after surgery in **Pt #1**, as shown by the reduction in serum creatinine levels, may have been influenced by improved glycemic function. However, renal improvement could be directly related to parathyroid adenoma resection because PHPT has long-term side effects such as kidney function decline. Although such progression typically occurs over time, the observed improvement suggests a possible acute benefit of adenoma removal. Also, renal improvement may enhance insulin resistance by restoring insulin clearance, reducing oxidative stress, and mitigating inflammation [20]. The correlation and causal relationship between renal and metabolic improvements after parathyroidectomy remain unclear and require further investigation.

In conclusion, our study emphasizes the clinical necessity of integrating FCH PET/CT and PVS into standard PHPT diagnostic algorithms by sensitively localizing with FCH PET/CT and detecting biochemical evidence from PVS. This combination will potentially improve diagnostic yield and long-term surgical outcomes through precise localization, although not all identified lesions are amenable to surgical removal. In addition, because there is no consensus on whether PTH induces or exacerbates insulin resistance, this remains an area for further research. Our study calls for future long-term studies on the effects of parathyroidectomy on glycemic and renal function, and the causal relationship between both functions postoperatively. Future studies should also explore the performance of alternative tracers, such as C11-methionine, in comparison with FCH.

Abbreviations

99mTc	Technetium-99 m
PTH	Parathyroid hormone
¹⁸ F	Fluorine 18
FCH PET/CT	Fluorine 18 fluorocholine positron emission tomography/computed tomography
PVS	Parathyroid venous sampling
PHPT	Primary hyperparathyroidism
MIBI	Sestamibi
SPECT	Single-Photon Emission Computed Tomography
DEXA	Dual-energy X-ray absorptiometry
SVC	Superior vena cava
EPA	Ectopic parathyroid adenoma
IJV	Internal jugular vein
BCV	Brachiocephalic vein
HOMA-IR	Homeostatic model assessment of insulin resistance
PHP1a	Pseudohypoparathyroidism type 1a

Acknowledgements

The authors thank all patients for their participation and Dr. Yoo Seung Chung for her insightful advice.

Author contributions

All authors made individual contributions to authorship. BJ, NH, SN and SiL were involved in the diagnosis and management of the patient. YS and SuL were involved in manuscript drafting. BJ, SN and SiL were involved in manuscript submission. All authors reviewed and approved the final draft.

Funding

This work was supported by the National Research Foundation of Korea (NRF) grant funded by the Korea government (MSIT) (2022R1A2C3006002 to SiL) and by the Gachon University research fund of 2024 (GCU- 202409780001 to SiL).

Data availability

Not applicable.

Declarations

Ethics approval and consent to participate

All procedures performed in the study involving human participants were in accordance with the ethical standards of the National Research committee and with the 1964 Helsinki Declaration and its later amendments or comparable ethical standards and informed consents to participate were provided by all patients.

Consent for publication

Signed informed consents for publication of clinical details and clinical images were obtained directly from all patients.

Competing interests

The authors declare no competing interests.

Received: 2 September 2025 / Accepted: 12 December 2025

Published online: 22 December 2025

References

1. Bilezikian JP, Bandeira L, Khan A, Cusano NE. Hyperparathyroidism. *Lancet*. 2018;391(10116):168–78.
2. Wareham NJ, Byrne CD, Carr C, Day NE, Boucher BJ, Hales CN. Glucose intolerance is associated with altered calcium homeostasis: a possible link between increased serum calcium concentration and cardiovascular disease mortality. *Metabolism*. 1997;46(10):1171–7.
3. Alexander RT, Hemmelgarn BR, Wiebe N, Bello A, Morgan C, Samuel S, et al. Kidney stones and kidney function loss: a cohort study. *BMJ*. 2012;345:e5287.
4. Udelsman R. Six hundred fifty-six consecutive explorations for primary hyperparathyroidism. *Ann Surg*. 2002;235(5):665–70, discussion 70–2.
5. Cheung K, Wang TS, Farrokhyar F, Roman SA, Sosa JA. A meta-analysis of preoperative localization techniques for patients with primary hyperparathyroidism. *Ann Surg Oncol*. 2012;19(2):577–83.
6. Kim WW, Lee Y-M, Sung T-Y, Chung K-W, Hong S-J. Selection of parathyroidectomy methods for primary hyperparathyroidism according to concordance between ultrasonography and MIBI scan results. *Gland Surg*. 2021;10(1):298–306.
7. Broos WAM, van der Zant FM, Knol RJJ, Wondergem M. Choline PET/CT in parathyroid imaging: a systematic review. *Nucl Med Commun*. 2019;40(2):96–105.
8. Kluijfhout WP, Pasternak JD, Gosnell JE, Shen WT, Duh Q-Y, Vriens MR, et al. ¹⁸F fluorocholine PET/MR imaging in patients with primary hyperparathyroidism and inconclusive conventional imaging: a prospective pilot study. *Radiology*. 2017;284(2):460–7.
9. Yamada T, Ikuno M, Shinjo Y, Hiroishi A, Matsushita S, Morimoto T, et al. Selective venous sampling for primary hyperparathyroidism: how to perform an examination and interpret the results with reference to thyroid vein anatomy. *Jpn J Radiol*. 2017;35(8):409–16.
10. Chan RK, Ruan DT, Gawande AA, Moore FD, Jr. Surgery for hyperparathyroidism in Image-Negative patients. *Arch Surg*. 2008;143(4):335–7.
11. Seib CD, Meng T, Suh I, Harris AHS, Covinsky KE, Shoback DM, et al. Risk of fracture among older adults with primary hyperparathyroidism receiving parathyroidectomy vs nonoperative management. *JAMA Intern Med*. 2022;182(1):10–8.
12. Liang CC, Yeh HC, Lo YC, Chou CY, Yen TH, Tsai HC, et al. Parathyroidectomy slows renal function decline in patients with primary hyperparathyroidism. *J Endocrinol Invest*. 2021;44(4):755–63.
13. Seib CD, Ganesan C, Furst A, Pao AC, Chertow GM, Leppert JT, et al. Estimated effect of parathyroidectomy on Long-Term kidney function in adults with primary hyperparathyroidism. *Ann Intern Med*. 2023;176(5):624–31.

14. Helman SN, Moubayed SP, Ho BT, Din-Lovinescu C, Urken ML. Parathyroid adenoma of the piriform sinus: case Series, embryologic Basis, and review of the literature. *AACE Clin Case Rep.* 2017;3(4):379–83.
15. Kim J, Cubangbang M, Adkins L, Chia S, DeKlotz TR, Boyle L, et al. Ectopic parathyroid adenoma in the pyriform sinus. *Head Neck.* 2017;39(10):E110–3.
16. Haap M, Heller E, Thamer C, Tschrüter O, Stefan N, Fritsche A. Association of serum phosphate levels with glucose tolerance, insulin sensitivity and insulin secretion in non-diabetic subjects. *Eur J Clin Nutr.* 2006;60(6):734–9.
17. Duran C, Sevinc B, Kutlu O, Karahan O. Parathyroidectomy decreases insulin resistance index in patients with primary hyperparathyroidism. *Indian J Surg.* 2017;79(2):101–5.
18. Nikooei Noghani S, Milani N, Afkhamizadeh M, Kabiri M, Bonakdaran S, Vazifeh-Mostaan L, et al. Assessment of insulin resistance in patients with primary hyperparathyroidism before and after parathyroidectomy. *Endocrinol Diabetes Metab.* 2021;4(4):e00294.
19. Muniyappa R, Warren MA, Zhao X, Aney SC, Courville AB, Chen KY, et al. Reduced insulin sensitivity in adults with pseudohypoparathyroidism type 1a. *J Clin Endocrinol Metab.* 2013;98(11):E1796–801.
20. Parvathareddy VP, Wu J, Thomas SS. Insulin resistance and insulin handling in chronic kidney disease. *Compr Physiol.* 2023;13(4):5069–76.

Publisher's note

Springer Nature remains neutral with regard to jurisdictional claims in published maps and institutional affiliations.